Estradiol Dose-Dependent Regulation of Membrane Estrogen Receptor-α, Metabotropic Glutamate Receptor-1a, and Their Complexes in the Arcuate Nucleus of the Hypothalamus in Female Rats

Matthew Mahavongtrakul, Martha P. Kanjiya, Maribel Maciel, Shrey Kanjiya, and Kevin Sinchak

Department of Biological Sciences, California State University, Long Beach, Long Beach, California 90840–9502

Sexual receptivity in the female rat is dependent on dose and duration of estradiol exposure. A 2 μg dose of estradiol benzoate (EB) primes reproductive behavior circuits without facilitating lordosis. However, 50 μg EB facilitates lordosis after 48 hours. Both EB doses activate membrane estrogen receptor-α (mERα) that complexes with and signals through metabotropic glutamate receptor-1a (mGluR1a). This mERα-mGluR1a signaling activates a multisynaptic lordosis-inhibiting circuit in the arcuate nucleus (ARH) that releases β-endorphin in the medial preoptic nucleus (MPN), activating μ-opioid receptors (MOP). MPN MOP activation is maintained, inhibiting lordosis for 48 hours by 2 μg EB, whereas 50 μg EB at 48 hours deactivates MPN MOP, facilitating lordosis. We hypothesized that 50 μg EB down-regulates ERα and mERα-mGluR1a complexes in the ARH to remove mERα-mGluR1a signaling. In experiment I, 48 hours after 2 μg or 50 μg EB, the number of ARH ERα-immunopositive cells was reduced compared with controls. In experiment II, compared with oil controls, total ARH ERα protein was decreased 48 hours after 50 μg EB, but the 2 μg dose was not. These results indicate that both EB doses reduced the total number of cells expressing ERα, but 2 μg EB may have maintained or increased ERα expressed per cell, whereas 50 μg EB appeared to reduce total ERα per cell. In experiment III, coimmunoprecipitation and Western blot revealed that total mERα and coimmunoprecipitated mERα with mGluR1a were greater 48 hours after 2 μg EB treatment vs rats receiving 50 μg EB. These results indicate 2 μg EB maintains but 50 μg EB down-regulates mERα-mGluR1a to regulate the lordosis circuit activity. **(*Endocrinology* 154: 3251–3260, 2013)**

Sexual receptivity (lordosis) in the rat is dependent on temporal integration of multiple estrogen receptor (ER) signaling pathways in neurocircuits that measure the dose and duration of estradiol exposure. A physiological dose of estradiol benzoate (EB; 2 μg) primes reproductive behavior circuits, but without subsequent progesterone does not facilitate lordosis (1). However, a larger EB dose (5–50 μg) facilitates lordosis after 48 hours (2, 3). In both cases, estradiol signaling through ERα is essential for reproductive behavior (4–8).

Although ERα is a classical transcription factor (9–14), recent studies have demonstrated that ERα is selectively palmitoylated and trafficked by site-specific caveolin proteins to the plasma membrane (mERα) and complex with and signal through metabotropic glutamate receptors (mGluR) (7, 15–18). In our model lordosis neurocircuit, estradiol rapidly signals through mERα complexed with mGluR1a that activates a multisynaptic circuit originating in the arcuate nucleus (ARH) (7, 19). This mERα-mGluR1a signaling induces proopiomelanocortin neu-

ISSN Print 0013-7227 ISSN Online 1945-7170
Printed in U.S.A.

Received March 12, 2013. Accepted June 20, 2013.
First Published Online July 3, 2013

Abbreviations: ARH, arcuate nucleus; CAV-1, caveolin-1; EB, estradiol benzoate; ER, estrogen receptor; GLB, gel-loading buffer; HYP, hypothalamus within the block; LIM, acronym of the 3 gene products Lin-11, Isl-1, and Mec-3; mERα, membrane estrogen receptor-α; mGluR, metabotropic glutamate receptor; MOP, μ-opioid receptor; MPN, medial preoptic nucleus; NGS, normal goat serum; PIC, protease inhibitor cocktail; PMSF, phenylmethanesulfonyl fluoride; SDS, sodium dodecyl sulfate; SNK, Student-Newman-Keuls; TBS, Tris-buffered saline; TRITC, tetramethylrhodamine isothiocyanate; VMHvl, ventromedial hypothalamus.

rons to release β-endorphin into the medial preoptic nucleus (MPN). MPN μ-opioid receptors (MOP) are activated and internalized, inhibiting lordosis (20). Initially, both 2 μg and 50 μg EB activate this inhibitory circuit, activating MPN MOP and inhibiting lordosis (1, 20). The priming dose of estradiol (2 μg EB) maintains MPN MOP activation and inhibits lordosis for 48 hours (2). In contrast, a 50 μg EB dose activates this circuit for at least 24 hours, and then by 48 hours MPN MOP are deactivated and lordosis is facilitated (2, 20). Antagonizing mGluR1a at the time of estradiol treatment blocks estradiol-induced sexual receptivity and MOP activation, indicating that mGluR1a signaling is necessary for estradiol-only facilitation of lordosis (7). Furthermore, antagonism of ERα with selective ER modulators (tamoxifen or ICI 182,780) 44 hours after 2 μg EB priming facilitates lordosis 4 hours later and decreases MOP activation (3).

These results suggest that ERα antagonism blocks mERα-mGluR1a signaling and removes the excitatory input to the β-endorphin neuron to reduce MOP activation. Because extended exposure to high doses of estradiol facilitates lordosis and down-regulates ERα in the hypothalamus (21, 22), we hypothesized that estradiol dose modulates trafficking of ERα to the membrane and the higher EB dose that facilitates lordosis and deactivates MPN MOP 48 hours after treatment does so through the down-regulation of ARH mERα-mGluR1a complexes and that 2 μg EB maintains ARH mERα-mGluR1a levels as a mechanism to maintain MOP activation and inhibition of lordosis. We also investigated whether these estradiol treatments differentially regulate nuclear and membrane ERα levels in the ARH.

Materials and Methods

General experimental design

Experiments I and II

Experiments I and II tested the hypothesis that down-regulation of ERα expression is dose dependently regulated by estradiol in the ARH, the remaining region of the hypothalamus within the block (HYP), and the amygdala. Ovariectomized rats were treated with oil, 2 μg EB, or 50 μg EB, and 48 hours later brains were collected to measure either the number of neurons that express ERα by counting ERα-immunopositive cells (experiment I) or to measure total ERα protein levels by Western blot analysis (experiment II).

Experiment III

Estradiol has been shown to regulate the trafficking of mERα in vitro (23). We tested the hypothesis that levels of mERα and mERα-mGluR1a complexes are regulated dose dependently by estradiol. Ovariectomized rats received oil, 2 μg EB, or 50 μg EB, and 48 hours later brains were collected and block dissected. Plasma membrane fractions were extracted and mERα and mGluR1a levels were determined by Western blot, and coimmunoprecipitation for mERα-mGluR1a complexes were performed and levels were measured by Western blot.

Animals. Adult Long-Evans rats (weighing 200–225 g) ovariectomized by the supplier (Charles River Laboratory Inc, Wilmington, Massachusetts) were used in all experiments. Animals were housed 2 females per cage and provided food and water ad libitum. All procedures for the experiments were reviewed and approved by the California State University, Long Beach, Institutional Animal Care and Use Committee.

Steroid treatment. One week after arrival, animals were given sc injections of safflower oil (oil group) or 2 μg EB once every 4 days or 50 μg EB once a week for 3 cycles (Sigma-Aldrich, St Louis, Missouri). The EB was dissolved in safflower oil so that the injection volume was 0.1 mL. Tissue collection procedures for each experiment were performed 48 hours after the third treatment.

Experiment I

Tissue collection

Animals were deeply anesthetized with isoflurane and transcardially perfused using cold 0.9% saline solution, followed by 4% paraformaldehyde in Sorensen's phosphate buffer (pH 7.4). Brains were postfixed and stored at 4°C overnight in the 4% paraformaldehyde. The brains were then transferred to 20% sucrose dissolved in a 0.1 M phosphate buffer solution (pH 7.5) for cryoprotection (24).

The brains were blocked and sectioned (20 μm) on a cryostat and then placed in a chamber filled with PBS (pH 7.5). The sections were collected using a paintbrush and placed in 24-well plates containing PBS. Each well contained 4 serial sections. The tissues were rinsed in chilled PBS 3 times for 5 minutes and then blocked with 10% methanol and 3% hydrogen peroxide in PBS for 10 minutes. The sections were then incubated with 0.2% Triton X-100 in PBS 3 times for 10 minutes, followed by a 30-minute incubation of 0.75% glycine in PBS. They were then incubated for 60 minutes in a blocking solution of 20% normal goat serum (NGS) and 1% BSA in PBS. The sections were then incubated in a polyclonal rabbit anti-ERα primary antiserum (1:10 000, C1355; Upstate Biotechnology Inc, Lake Placid, New York) in 1% NGS in PBS for 2 nights at 4°C. After the incubation, the sections were washed 3 times for 10 minutes in PBS, and once for 10 minutes in Tris-buffered saline (TBS). This was followed by incubation with tetramethylrhodamine isothiocyanate (TRITC)-labeled goat antirabbit secondary antiserum at a concentration of 1:200 with 1% NGS in chilled TBS for 2 hours at room temperature and covered to avoid bleaching of the fluorescent labels (Jackson ImmunoResearch Laboratories, West Grove, Pennsylvania). Finally, the sections were washed 3 times for 5 minutes in TBS and once for 5 minutes in 0.1 M Tris buffer (pH 7.5) before mounting. The slides were dried on a slide warmer at 37°C and coverslipped with Aqua-Poly Mount (Polysciences, Warrington, Pennsylvania).

Analysis of ERα-immunopositive cell counts

Images of ERα immunofluorescence labeling were captured using the Leica DM6000 epiluminescent microscope, Leica DFC 360FX monochrome digital camera, and Leica AF-LAS microscope software through a TRITC filter cube (Leica, Heidelberg, Germany). ERα TRITC labeling was visualized by imaging at a 649-nm emission filter and a 620- to 660-nm band pass filter. The captured images were imported to ImageJ software (National Institutes of Health, Bethesda, Maryland) for analysis and adjusted for brightness and contrast. A cell counter plug-in in ImageJ was used to count the number of cells in the ARH, amygdala, and ventromedial hypothalamus (VMHvl) that were ERα immunopositive in each of the 3 treatments. A mean from a minimum of 4 sections per area per animal was calculated and means for each steroid treatment were calculated. A 1-way ANOVA analyzed the effects of EB treatment on ERα-positive cell number, followed by the Student-Newman-Keuls (SNK) post hoc analysis.

Experiments II and III

Tissue collection

Forty-eight hours after the third steroid treatment, the animals were deeply anesthetized with isoflurane and killed by decapitation. Brains were removed from the cranium and chilled in PBS at 4°C, and block dissections of the ARH, remaining HYP, and amygdala were performed (Figure 1). The block dissections were rapidly frozen by placing them individually in a microcentrifuge tube and submerging the tube in a dry ice and ethanol bath and were stored at −80°C until processing for protein extraction and Western blot analysis (experiment II) or plasma membrane extraction and coimmunoprecipitation (experiment III).

Total protein extraction. For Western blot analysis, the brain tissues were individually homogenized using a glass tissue grinder, and total protein was extracted (Kimble Chase, Vineland, New Jersey). The tissue lysates were stored in 2× gel-loading buffer [GLB; 0.5 M Tris, pH 6.8; 10% (wt/vol) sodium dodecyl sulfate (SDS), 20% glycerol] containing a 1:10 dilution of protease inhibitor cocktail (PIC; Sigma-Aldrich) and a 1:100 dilution of phenylmethanesulfonyl fluoride (PMSF; Sigma-Aldrich). Samples of the protein were obtained by centrifuging the tubes at 10 000 × *g* for 5 minutes at 4°C and discarding the pellet; these samples were analyzed using the bicinchoninic acid assay (Thermo Pierce, Rockford, Illinois); the rest were stored at −80°C until processing. Total concentration of protein was determined using UV-visible spectrophotometry at a 562-nm wavelength (Bio-Rad Laboratories, Hercules, California).

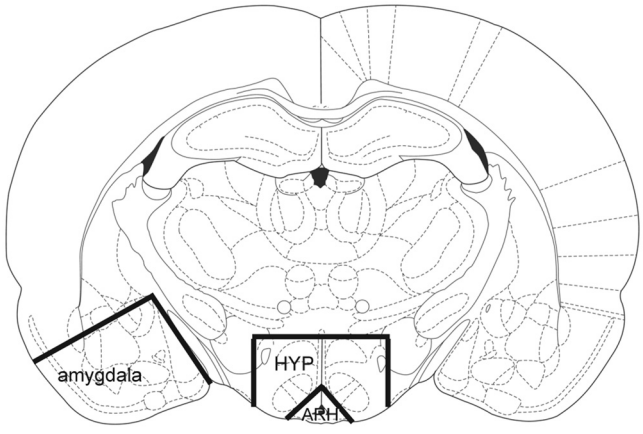

Figure 1. Representative coronal section showing the approximate midlevel region of block dissection (bregma −2.80) and boundaries of the arcuate nucleus, hypothalamus (excluding the ARH), and amygdala used in experiments II and III (52).

Plasma membrane protein extraction. In preparation for plasma membrane analysis and coimmunoprecipitation, plasma membrane fractions were extracted from the ARH using the plasma membrane protein extraction kit (Abcam, Cambridge, Massachusetts). To obtain enough protein for analysis, 4 ARH samples were pooled for each analyzed sample. Briefly, ARH tissue were suspended in homogenization buffer containing PIC (1:500, supplied with the kit), homogenized with a glass tissue grinder, and centrifuged at 700 × *g* for 10 minutes at 4°C (Kimble Chase). The pellet was discarded and the supernatant was centrifuged at 10 000 × *g* for 30 minutes at 4°C. This step separated the cytosolic fraction from the membrane fraction. The pellet (containing the plasma membrane and organelle membrane fractions) was subject to extraction with various reagents (provided with the kit). After the final centrifugation, the purified plasma membrane fraction was resuspended in 100 μL of 2× GLB containing PIC (1:10) and PMSF (1:100). After the extractions were complete, the extracts were subjected to the bicinchoninic acid assay as described previously. Absence of mitochondrial contamination was confirmed using a succinate dehydrogenase assay, and absence of cytosolic contamination and presence of membrane were confirmed by Western blots against the cytosolic marker LIM (acronym of the 3 gene products Lin-11, Isl-1, and Mec-3) kinase-1 and the membrane marker flotilin-1, respectively.

Western blot. Twenty-micrograms samples of protein from the total protein extracts were thawed on a 95°C heat block for 5 minutes, combined with 5% β-mercaptoethanol and 45% 2× Laemmli buffer, and run on a SDS-PAGE gel (4% stacking gel: 30% degassed acrylamide; 0.5 M Tris-HCl, pH 6.8; 10% (wt/vol) SDS, containing ammonium persulfate and N,N,N′,N′-tetramethylethylenediamine; and 8% resolving gel: 30% degassed acrylamide; 1.5 M Tris-HCl, pH 8.8; 10% (wt/vol) SDS, containing ammonium persulfate and N,N,N′,N′-tetramethylethylenediamine) for 1 hour 20 minutes at room temperature in 1× running buffer (tris, glycine, and SDS). The stacking gel was removed, and the resolving gel was placed in a transfer module (Bio-Rad Laboratories). To transfer the protein from the SDS-PAGE gel to nitrocellulose membranes, the transfer module was placed in transfer buffer (methanol, Tris, and glycine), and 100 V was passed across the module for 2 hours at 4°C. Successful transfer of protein to the membranes was confirmed using a removable Ponceau S staining solution on the membranes and a coomassie blue stain on the gels (Fisher Scientific, Fair lawn, New Jersey). The membranes were blocked with 10% nonfat milk overnight at 4°C on an orbital shaker (LabScientific Inc, Livingston, New Jersey). The next day, the membranes were incubated overnight at 4°C on an orbital shaker with affinity-purified rabbit anti-ERα (1:500 in 5% nonfat milk, MC-20; Santa Cruz Biotechnology, Santa Cruz, California), mouse anti-mGluR1a (1:500; BD Pharmingen, San Diego, California), mouse anti-β-actin (1:20 000 in 5% nonfat milk; Sigma-Aldrich), rabbit

anti-LIM kinase-1 (1:1000; Abcam), or rabbit antiflotillin-1 (1:1000; Abcam) primary antiserum. The following day, the membranes were washed 3 times with 1× TBS with 0.1% Tween 20 for 20 minutes each and then incubated with an affinity-purified peroxidase-conjugated goat antirabbit secondary antiserum (1:10 000; Sigma-Aldrich) or rabbit antimouse secondary antiserum (1:50 000; Sigma-Aldrich) for 45 minutes at room temperature on an orbital shaker. This was followed by 3 washes with 1× TBS with 0.1% Tween 20 for 30 minutes each. The membranes were then incubated in West Pico chemiluminescent substrate (1:1 ratio of luminol and peroxide) for 5 minutes and then placed in a cassette and imaged with Biomax light film in the dark to visualize bands (Thermo Scientific).

Coimmunoprecipitation. One hundred-microgram samples of protein from the plasma membrane extraction were immunoprecipitated using Protein A/G Plus agarose beads (Santa Cruz Biotechnology). Briefly, the lysate was precleared by adding 1.0 μg of normal rabbit serum with 20 μL beads and incubated on a tube rotator at 4°C for 30 minutes (Thermo Scientific). The precleared lysate was then centrifuged at 1000 × *g* for 5 minutes at 4°C, and the supernatant was transferred to a new tube containing 2 μg mouse anti-mGluR1a primary antiserum (BD Pharmingen). After 1 hour incubation at 4°C on the tube rotator, 20 μL beads was added to the tube and incubated at 4°C overnight on a rotator. The following day, the beads were washed 4 times with 1× PBS, each time being centrifuged at 1000 × *g* at 4°C. After the final wash, the beads were resuspended in 40 μL 2× GLB containing PIC (1:10) and PMSF (1:100).

After resuspension, the beads were placed on a 95°C heat block for 5 minutes and then centrifuged at 1000 × *g* for 5 minutes to elute the protein. This elution was run on a SDS-PAGE gel and blocked as described previously. The membrane was then incubated overnight at 4°C on the orbital shaker with affinity-purified rabbit anti-ERα primary antiserum (1:500 in 5% nonfat milk, MC-20; Santa Cruz Biotechnology) or mouse anti-mGluR1a primary antiserum (1:500; BD Pharmingen). For Western blot analysis of this experiment, a rabbit antimouse secondary antiserum (1:50 000; Sigma-Aldrich) or a conformation-specific mouse antirabbit secondary antiserum was used (Cell Signaling, Beverly, Massachusetts). The membrane was then developed as described previously.

Analysis. Densitometry of the Western blots was obtained with the Quantity One software (Bio-Rad Laboratories). The film was imaged using a Gel Doc XR charge-coupled device camera (Bio-Rad Laboratories). For whole tissue and plasma membrane Western blot analysis, bands were normalized to β-actin and flotillin-1, respectively. For each of the experimental groups, a mean normalized intensity was calculated. Then the normalized intensities were divided by the mean normalized intensity. For the control animals, this resulted in a normalized average of 1.0, allowing for comparison of all of the experimental group means relative to 1.0. Relative changes in coimmunoprecipitation density for mERα levels were calculated by dividing the mERα levels by the mGluR1a levels within the same treatment group. These densities were then divided by the density of the oil group, allowing for relative comparisons of the treatment groups relative to 1.0.

Whole tissue and plasma membrane Western blots were analyzed by 1-way ANOVA with a significance threshold of $P < .05$ followed by SNK or Tukey's post hoc test. All statistical analyses were done using SigmaStat 3.5 (Systat Software, San Jose, California).

Results

Experiment I

Both 2 μg and 50 μg EB reduced ERα-immunoreactive positive cells in the ARH

In all regions analyzed, ERα-positive immunoreactivity was localized to the nucleus of the cell (Figure 2). Although we demonstrate in experiment III the presence of mERα, our immunohistochemical analysis did not stain mERα (Figure 2). Forty-eight hours after the final injections, both the 2 μg and 50 μg EB doses decreased the number of ERα-immunopositive cells in the ARH (Figure 2F); 1 way ANOVA df = 2,14, F = 15.744, $P < .001$; n = 4–6 animals per group; SNK post hoc test, $P < .05$), but neither dose had an effect on the number of ERα-immunopositive neurons in the VMHvl or posterodorsal medial amygdala when compared with oil controls (Figure 2F (Table 1); VMHvl: 1 way ANOVA df = 2,65, F = 1.81, $P = .171$; posterodorsal medial amygdala: 1 way ANOVA df = 2,30, F = 1.51, $P = .237$).

Experiment II

The 50 μg EB dose down-regulated total ERα protein levels in the ARH and HYP but not in the amygdala

To test whether 2 μg or 50 μg EB down-regulates total ERα protein levels, total protein was extracted from freshly collected block dissections of ARH, HYP, and amygdala tissue. In the ARH and HYP, 50 μg EB down-regulated total ERα protein levels compared with oil-treated rats (Figure 3, A and B; ARH: 1 way ANOVA df = 2,14, F = 3.93, $P = .049$; n = 5 animals per group; HYP: 1 way ANOVA df = 2,13, F = 4.078, $P = .047$; n = 4–5 animals per group; Tukey's post hoc test, $P < .05$). In both the ARH and HYP, the 2 μg EB dose was intermediate between the oil- and 50 μg EB-treated groups (Tukey's post hoc test, $P < .05$). Neither EB dose affected total ERα protein levels in the amygdala (Figure 3C; 1 way ANOVA df = 2,14, F = 0.10, $P = .908$; n = 5 animals per group).

Measuring both the number of ERα-immunopositive cells and total ERα protein expression revealed a site-specific and dose-dependent estradiol regulation of ERα. These results from experiments I and II suggest that although 2 μg EB decreases the number of ERα-immunopositive cells, the amount of ERα per cell is maintained or increased because total ERα protein remains elevated in the ARH after 48 hours. In contrast, 50 μg EB decreased

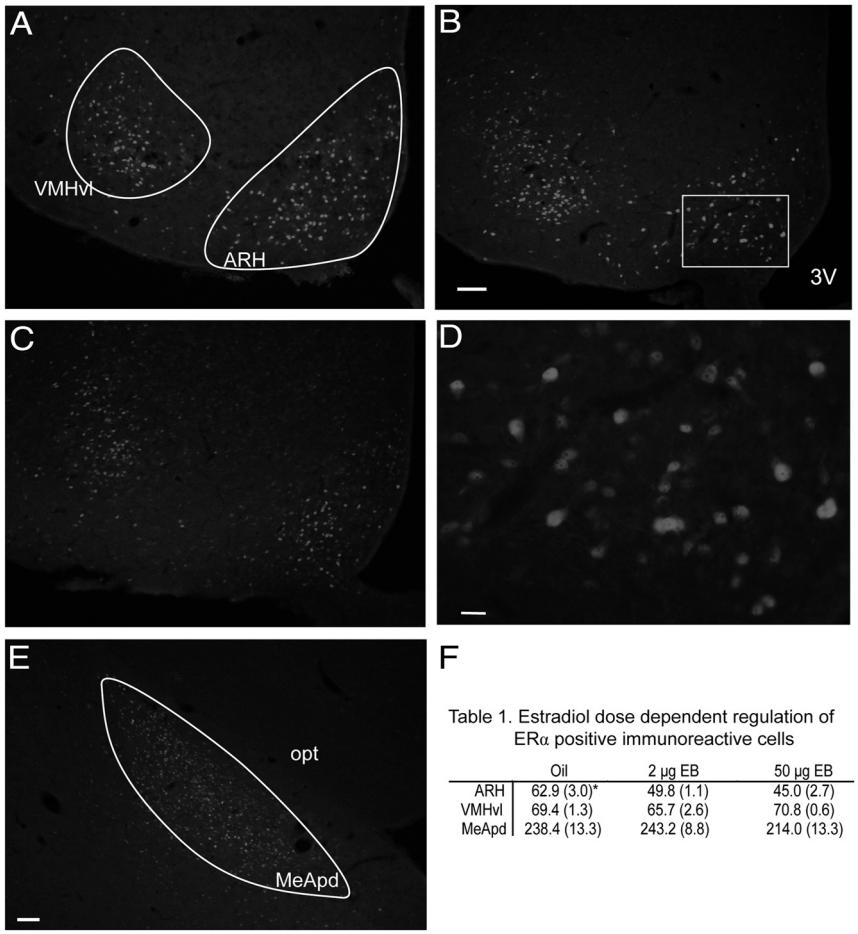

Table 1. Estradiol dose dependent regulation of ERα positive immunoreactive cells

	Oil	2 μg EB	50 μg EB
ARH	62.9 (3.0)*	49.8 (1.1)	45.0 (2.7)
VMHvl	69.4 (1.3)	65.7 (2.6)	70.8 (0.6)
MeApd	238.4 (13.3)	243.2 (8.8)	214.0 (13.3)

Figure 2. Representative photomicrographs of ERα TRITC immunofluorescent-positive cells in the ARH, VMHvl, and medial amygdala posterodorsal (MeApd). ER immunofluorescent-positive cells were counted in oil- (A), 2 μg EB- (B), or 50 μg EB (C)-treated ovariectomized rats in the ARH and VMHvl. D, Photomicrograph of the outlined region in panel B illustrating the ERα immunostaining is mainly associated with the nucleus. E, Representative section of the medial amygdala posterodorsal (MeApd) region in which ERα-immunopositive cells were counted. F, Table 1, ERα-immunopositive mean cell counts (SEM) in ovariectomized rats 48 hours after treatment with Oil, 2 μg EB, or 50 μg EB in the ARH, VMHvl, and MeApd. *, Significantly different from other EB groups within the brain region; SNK $P < .05$. opt, optic tract; 3V, third ventricle. Scale bar, 50 μm (A and E), 10 μm (D).

both the amount of ERα-immunopositive cells as well as total protein levels, indicating an overall down-regulation of ERα. Because the 2 μg EB dose appeared to increase the amount of ERα expressed per cell, whereas the 50 μg EB dose down-regulated ERα levels, we tested whether the estradiol dose regulated mERα-mGluR1a levels in experiment III.

Experiment III

The 50 μg EB dose down-regulated plasma membrane ERα protein levels in the ARH

To determine whether the dose-dependent regulation of ERα occurs in a manner important for plasma membrane signaling, plasma membrane fractions were extracted from ARH tissue. Absence of cytosolic contamination and presence of membrane fractions were confirmed using Western blots against the cytosolic marker LIM kinase-1 and the membrane marker flotillin-1, respectively (Figure 4A). Absence of mitochondrial contamination was confirmed using a succinate dehydrogenase assay (data not shown). Plasma membrane ERα protein levels in the 2 μg EB group were significantly higher than the oil and 50 μg EB groups (Figure 4C; df = 2,9, F = 13.00, $P = .004$; n = 3–4 pools of 8 animals per group; SNK post hoc test, $P < .01$). However, the 50 μg EB group was not significantly different from the oil group (SNK, oil vs 50 μg EB, $P = .516$). In contrast, Western blot analysis revealed no estradiol regulation of plasma membrane mGluR1a protein levels (Figure 4D; 1 way ANOVA df = 2,13, F = 0.111, $P = .896$; n = 4–5 pools of 8 animals per group).

The 2 μg EB dose increased ARH mERα-mGluR1a complexes, whereas 50 μg EB down-regulated these complexes

Previous in vitro studies have shown that mERα complexes with and signals through mGluR1a to modulate sexual receptivity (7). To determine whether levels of mERα-mGluR1a complexes in vivo are regulated by estradiol in a behaviorally relevant manner, coimmunoprecipitation was done on plasma membrane extracts from ARH tissue. The mGluR1a was immunoprecipitated from ARH plasma membrane extracts, which were then probed by Western blot for ERα and mGluR1a in series, and ERα level was relatively compared with mGluR1a density (Figure 5). The mERα-mGluR1a complex levels were regulated by estradiol dose. Both oil- and 50 μg EB-treated animals had low levels of mERα-mGluR1a complexes. The 2 μg EB treatment group had a 1.5-fold increase in the amount of mERα-mGluR1a complexes compared with both other treatment groups (Figure 5).

Discussion

The present study demonstrates that estradiol differentially regulates the expression, trafficking, and complex-

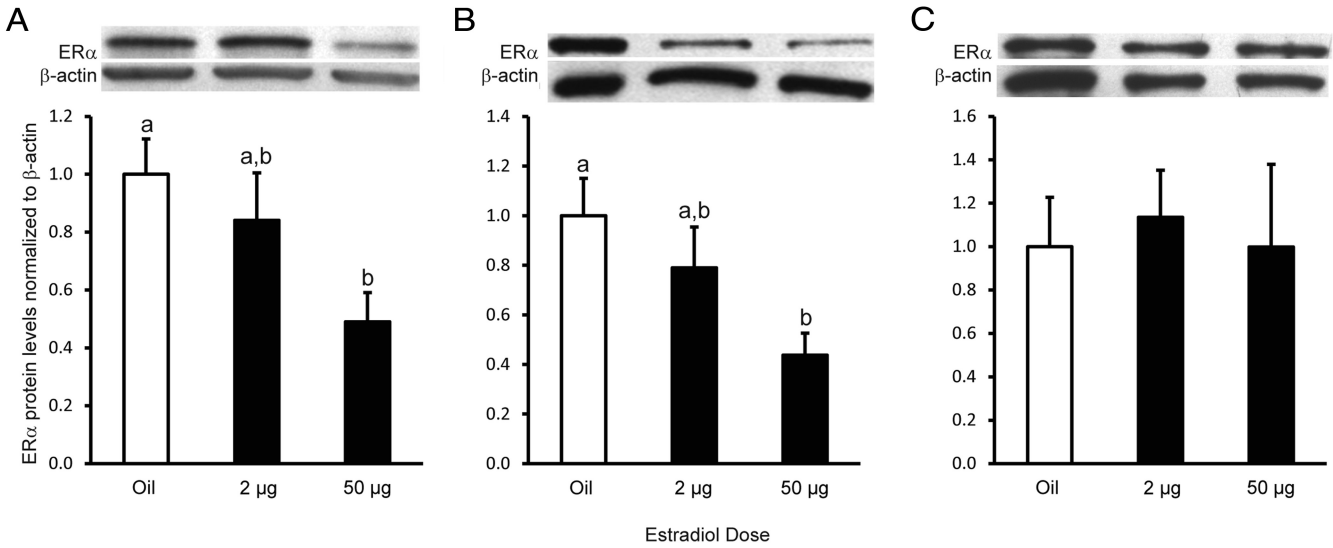

Figure 3. Estradiol dose-dependent regulation of total ERα protein levels in the ARH, HYP, and amygdala. A–C, Western blot analysis and graphical representation of total ERα protein levels in the ARH (A), remaining HYP (B), and whole amygdala (C). Total protein was extracted from the ARH, remaining HYP, and amygdala, and 20 μg was run on a SDS-PAGE gel and probed for ERα and normalized to β-actin. In both the ARH and remaining HYP, 50 μg EB down-regulated total ERα protein levels compared with oil-treated animals, whereas the 2 μg EB dose had intermediate total ERα protein levels between the oil and 50 μg EB groups. There was no effect of EB treatment on ERα total protein levels in the amygdala. Treatments with different letters indicate significant differences in ERα protein levels (Tukey's post hoc analysis, $P < .05$).

ing of ERα to mGluR1a, providing potential mechanisms for regulation of multiple ERα signaling pathways. Furthermore, estradiol regulates mERα and mERα-mGluR1a levels in the ARH to regulate membrane estrogenic signaling in a dose-dependent and behaviorally relevant manner. In vitro, mERα levels are rapidly regulated by estradiol (23, 25). However, the present experiments demonstrate that estradiol dosage regulates in vivo levels of ARH mERα and mERα-mGluR1a complexes important for estradiol regulation of the ARH-MPN lordosis inhibitory circuit 48 hours after treatment, a time point that is associated with the facilitation of sexual receptivity. Initially, both the low priming dose (2 μg) and higher doses (5–50 μg) of EB rapidly activate mERα-mGluR1a complexes in the ARH to induce β-endorphin release, activate MPN MOP, and inhibit lordosis (3, 7, 19, 20). Our present results indicate that the continuous MPN MOP activation for 48 hours by 2 μg EB is through the up-regulation and maintenance of mERα-mGluR1a complexes in the ARH, which inhibits lordosis. In contrast, MPN MOP are deactivated at 48 hours by 5–50 μg EB, facilitating lordosis (2, 7, 20). The present mERα experiments reveal a down-regulation of ARH mERα and mERα-mGluR1a complexes 48 hours after 50 μg EB treatment compared with the 2 μg EB dose (Figures 4 and 5). This mERα down-regulation may reduce estradiol excitatory signaling to β-endorphin neurons that project to the MPN (3, 7, 20, 26). Previous studies indicate that regulation of mERα signaling may modulate the rapid sustained activation and the delayed inactivation of the ARH-MPN lordosis-inhibitory circuit (3, 20). Our present data provide evidence that these actions are regulated by mERα-mGluR1a signaling that is modulated by estradiol dose.

Others have shown estradiol regulation of ERα using individual markers of expression (eg, in situ hybridization, immunocytochemistry, autoradiography; 21, 22, 27–32). Our immunohistochemical results demonstrate that nuclear ERα is down-regulated by both doses of EB. ERα immunohistochemistry studies report and quantify ERα staining that is localized to the nucleus with little or no cytosolic or membrane staining [(33, 34) and Figure 2]. Thus, the increased trafficking of ERα to the membrane by 2 μg EB may reduce the levels of nuclear ERα below levels of detection by immunohistochemistry but still detected by Western blot. However, measuring ARH ERα immunopositive cell number, total ERα, mERα, and mERα-mGluR1a complexes allows for greater insight into regulation of ERα expression and trafficking that controls the multiple ERα signaling mechanisms within neurons. Measuring total ERα in similarly treated animals revealed potential changes in ERα trafficking that is not revealed with immunohistochemistry alone. For example, although 48 hours after 2 μg EB the number of ARH ERα-immunopositive neurons are decreased, total ERα was not changed, suggesting the amount of ERα per cell is maintained or increased. This is supported by the increased levels of mERα and mERα-mGluR1a complexes. Furthermore, although both the 2 μg and 50 μg EB doses down-regulate nuclear ERα immunostaining, this priming dose of 2 μg EB increased the levels of mERα-mGluR1a com-

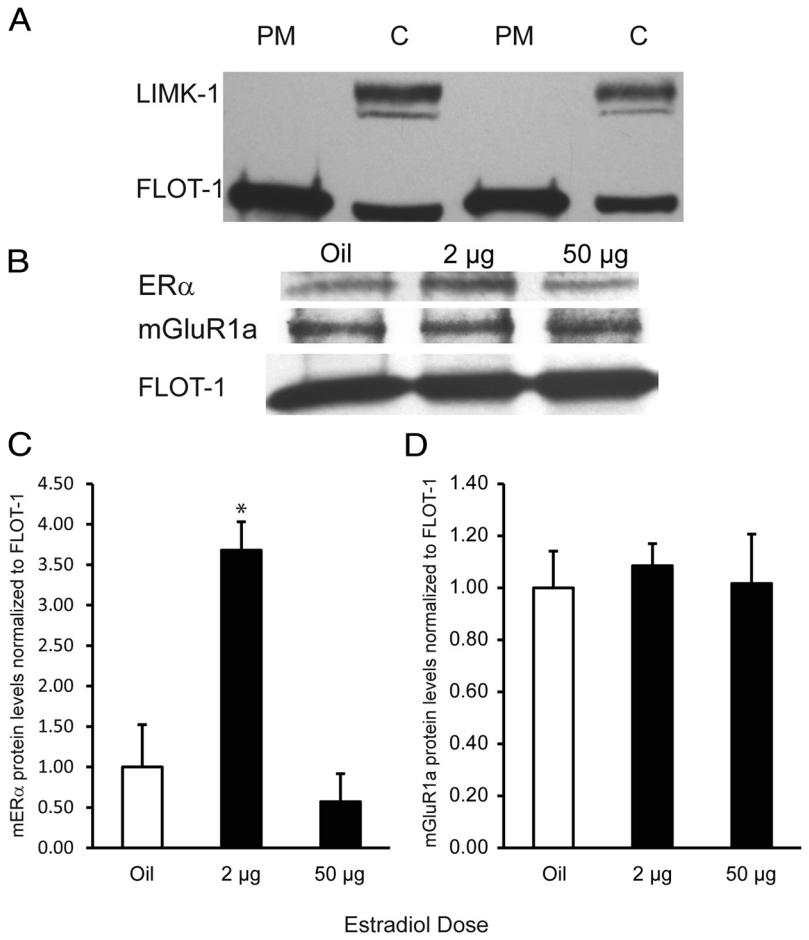

Figure 4. Estradiol regulation of plasma membrane ERα protein levels in ARH. A, Representative Western blot showing absence of cytosolic (C) contamination in plasma membrane (PM) preparations. Twenty micrograms of plasma membrane preparations were loaded onto a SDS-PAGE gel and probed for the cytosolic marker LIM kinase-1 (LIMK-1) or the membrane marker flotillin-1 (FLOT-1). Western blot analysis (B) and graphical representation of plasma membrane ERα (panel C) and mGluR1a (panel D) in the ARH. Plasma membrane fractions were obtained from ARH tissue, and 20 μg was loaded onto a SDS-PAGE gel and probed for ERα and mGluR1a. Levels were normalized to flotillin-1. Forty-eight hours after treatment, the 2 μg EB group up-regulated membrane ERα protein levels relative to the oil group, whereas the 50 μg EB appears to have down-regulated plasma membrane ERα protein levels relative to the 2 μg EB group by 48 hours after treatment. There was no effect of EB treatment on mGluR1a plasma membrane levels in the ARH. *, Significantly greater than oil and 50 μg EB.

pared with the 50 μg EB-treated rats and Oil-treated controls. Thus, mERα-mGluR1a signaling is up-regulated and maintained 48 hours after estradiol priming in a subset of ARH neurons that may allow for the continued excitation/activation of the β-endorphin neurons projecting to the MPN to maintain the inhibition of lordosis.

In contrast, 48 hours after treating with 50 μg EB, all measures of ARH ERα were reduced. This included the number of ERα immunopositive cells, total mERα, and mERα-mGluR1a complexes. Thus, the 50 μg EB dose at 48 hours may be acting through 2 mechanisms that reduce the activity of the β-endorphin neuron to facilitate lordosis: 1) removing excitatory input to the β-endorphin neuron through reduction in mERα-mGluR1a signaling on the plasma membrane, and 2) increasing inhibitory input through release of orphanin FQ (also known as nociceptin) to activate opioid receptor-like receptor-1 that signals through G protein-coupled inward-rectifying potassium channels to inhibit β-endorphin output and deactivate MPN MOP (2, 35, 36).

In vitro, estradiol rapidly increases ERα trafficking to the plasma membrane, internalization from the membrane, and recycling back to the plasma membrane (25, 37). The present results indicate that the dose of estradiol regulates both the trafficking of ERα to the plasma membrane and the formation of mERα-mGluR1a complexes in the ARH 48 hours after treatment. The 2 μg EB dose increased these complexes compared with the oil-treated animals. In contrast, 48 hours after 50 μg EB, mERα levels were reduced compared with 2 μg EB and were similar to levels in the oil-treated group. Furthermore, the dose of estradiol also appears to induce and regulate the formation of mERα-mGluR1a complexes in the ARH. mERα was present in oil-treated animals, and the coimmunoprecipitation experiment revealed a basal level of mERα-mGluR1a. The priming 2 μg EB dose increased the levels of mERα-mGluR1a complexes 1.5-fold compared with oil-treated animals. mERα-mGluR1a levels in the 50 μg EB group were equivalent to oil-treated animals. Because both EB doses initially activate MPN MOP (7, 20), it is likely that both EB doses initiate the trafficking of ERα to the membrane.

The exact signal to increase mERα levels is unclear. Simply overexpressing ER (ERα or ERβ) in Chinese hamster ovary cells increases mER levels, indicating that ER intracellular levels may regulate ER trafficking to the plasma membrane (38). Additionally, estradiol rapidly increases the ERα trafficking, internalization, and recycling to the plasma membrane (25, 37). Thus, mERα trafficking mechanisms appear to be regulated in part by ER expression levels and exposure to estradiol.

The site-specific trafficking of ERα to the membrane and interaction with particular mGluRs is dependent on

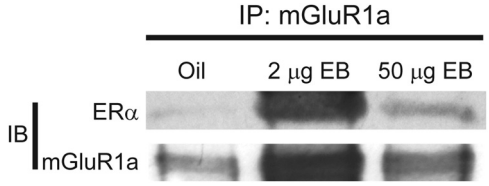

Figure 5. Estradiol regulation of mERα-mGluR1a complexes on the plasma membrane in the ARH. Plasma membrane fractions were extracted from ARH tissue, and 100 μg was immunoprecipitated with mGluR1a (IP) and probed for ERα and mGluR1a (IB). Because plasma membrane mGluR1a protein levels were not affected by EB treatment, the amount of ERα that coimmunoprecipitated with mGluR1a was compared in a relative manner across the treatment groups. Oil-treated animals had low basal mERα-mGluR1a complexes, whereas 2 μg EB induced a 1.5-fold increase in mERα-mGluR1a complexes on the plasma membrane in the ARH. The 50 μg EB group had mERα-mGluR1a complex levels that were equivalent to the oil group.

specific caveolin proteins (39). Caveolae communicate with the cell surface and are important for vesicular transport and clustering of intracellular signaling proteins (40, 41). These caveolae form pits in the membrane that represent either exocytotic vesicular fusion delivering ERα to the membrane or endocytotic vesicular fusion that internalizes and removes ERα from the membrane (42–45). Caveolin-1 (CAV-1) is associated with mERα trafficking and association with mGluR1a in the hypothalamus (8, 39, 46–48). Knockdown of CAV-1 using small interfering RNA reduces mERα levels (8, 39). Furthermore, removal of CAV-1 expression in the ARH in vivo blocks the estradiol signaling that activates MPN MOP and facilitates lordosis (8). This removal of CAV-1 in vivo had similar effects to blocking mGluR1a activation at the time of high estradiol treatment: blocking estradiol induced MPN MOP activation and facilitation of lordosis (7). These CAV-1-ERα interactions are palmitoylation dependent. Palmitoylation of ERα in the nucleus allows it to be associated with CAV-1 and trafficked to the plasma membrane. In contrast, the 50 μg EB dose may induce the depalmitoylation of mERα and the dissociation of mERα from CAV-1 to down-regulate mERα at 48 hours (8, 39, 46–48). Our data suggest that both EB doses initially increase the activity of these trafficking mechanisms to permit mERα-mGluR1a signaling.

The maintenance of mERα-mGluR1a levels appears dependent on estradiol dose. The 2 μg dose appears to maintain ERα trafficking to the membrane, whereas the 50 μg dose has a delayed down-regulation of mERα at 48 hours. The estradiol regulation of ERα trafficking to and from the membrane has been shown in vitro using biotinylation studies (25). Initially, ERα is rapidly and transiently trafficked to the cell surface 30 minutes after estradiol exposure. At this time point, however, biotinylated ERα was also observed in the cytoplasm. This is consistent with the idea that mERα-mGluR1a complexes are internalized into early endosomes characteristic of activated G protein-coupled receptors. These receptors can be either recycled back to the membrane or targeted for degradation (25, 37).

Our in vivo data support in vitro findings that estradiol increases mERα and does not alter membrane mGluR1a levels (25). However, in vitro mERα are rapidly removed from the membrane, whereas our results in vivo indicate that these mERα-mGluR1a complexes are up-regulated and maintained by the priming dose of estradiol. The maintenance of mERα-mGluR1a in vivo is likely occurring through recycling and palmitoylation-initiated mechanisms compared with the rapid internalization and reduction in vitro (23, 25, 37). The high dose of EB likely recycles mERα for at least 24 hours because MPN MOP activation is maintained during this period. However, by 48 hours the trafficking of ERα to the membrane is reduced and mERα-mGluR1a signaling is reduced as indicated by MPN MOP deactivation (2, 20). Although the mechanism is unclear, the estradiol dose and exposure is measured to regulate the expression and trafficking of ERα. One way that estradiol dose and duration appears to be measured is through ARH mERα-mGluR1a signaling. Antagonizing mGluR1a prior to a high dose of estradiol treatment blocked the facilitation of lordosis when compared with rats that received estradiol only (7).

Conversely, concurrent infusion with a mGluR1a agonist with estradiol priming facilitated lordosis as if the animals were treated with a high dose of estradiol (7). It is possible that mERα-mGluR1a interact with other intracellular/genomic mechanisms to measure estradiol dose and duration to modulate ERα expression and trafficking. In the intact rat, the ability to measure circulating levels and time of exposure may be localized within multiple neural pathways to regulate sexual receptivity associated with her reproductive life history. For example, during early menopause, circulating estradiol levels are elevated and remain elevated, exposing the brain to levels of estradiol that are mimicked by 50 μg EB (49). At this point, she is continuously sexually receptive and has become a reflex ovulator, in which copulation with a male induces the LH surge and ovulation (50). In the rat with regular estrous cycles, ovulation is spontaneous. However, the circulating estradiol levels, which are mimicked by the 2 g EB dose, are not adequate to facilitate sexual receptivity without progesterone from the ovary (51). Thus, estradiol regulation of ARH mERα-mGluR1a levels may be part of the mechanism that regulates and coordinates her sexual receptivity with the state of her reproductive cycle.

The present study demonstrates that mERα and mERα-mGluR1a levels in the ARH are regulated in a dose-dependent manner by estradiol that could regulate estradiol

signaling important for modulating activity of neurocircuits. This regulation of membrane initiated estradiol signaling may affect the activity of reproductive and energy balance neurocircuits across the estrous cycle (reviewed in Reference 35). In the ARH-MPN lordosis-inhibitory model circuit, priming levels of estradiol up-regulate mERα-mGluR1a levels, allowing for the maintenance of MPN MOP activation and inhibition of lordosis to prevent copulation. In contrast, higher doses of estradiol that facilitate lordosis reduce mERα-mGluR1a signaling and remove excitatory input to the β-endorphin neurons to alleviate inhibition of behavior through MPN MOP.

Acknowledgments

We thank Dr Houng-Wei Tsai, Dr Eric Haas-Stapleton, and Dr Roger Acey for technical assistance.

Address all correspondence and requests for reprints to: Kevin Sinchak, PhD, Department of Biological Sciences, 1250 Bellflower Boulevard, California State University, Long Beach, Long Beach, California 90840–9502. E-mail: kevin.sinchak@csulb.edu.

This work was supported by National Institutes of Health awards RO1HD058638 from the *Eunice Kennedy Shriver* National Institute of Child Health and Human Development (to K.S.) and Research Initiative for Science Enhancement Award GM07163 at California State University, Long Beach.

Disclosure Summary: The authors have nothing to disclose.

References

1. **Sinchak K, Micevych PE.** Progesterone blockade of estrogen activation of μ-opioid receptors regulates reproductive behavior. *J Neurosci*. 2001;21(15):5723–5729.
2. **Sanathara NM, Moraes J, Kanjiya S, Sinchak K.** Orphanin FQ in the mediobasal hypothalamus facilitates sexual receptivity through the deactivation of medial preoptic nucleus μ-opioid receptors. *Horm Behav*. 2011;60(5):540–548.
3. **Garcia BL, Mana A, Kim A, Sinchak K.** Antagonism of estrogen receptors facilitates sexual receptivity through opioid circuits in the arcuate nucleus of the hypothalamus and the medial preoptic nucleus in estradiol primed non-receptive female rats. Paper presented at: 40th Meeting of the Society for Neuroscience; November 2010; San Diego.
4. **Lubahn DB, Moyer JS, Golding TS, Couse JF, Korach KS, Smithies O.** Alteration of reproductive function but not prenatal sexual development after insertional disruption of the mouse estrogen receptor gene. *Proc Natl Acad Sci USA*. 1993;90(23):11162–11166.
5. **Ogawa S, Taylor JA, Lubahn DB, Korach KS, Pfaff DW.** Reversal of sex roles in genetic female mice by disruption of estrogen receptor gene. *Neuroendocrinology*. 1996;64(6):467–470.
6. **Ogawa S, Eng V, Taylor J, Lubahn DB, Korach KS, Pfaff DW.** Roles of estrogen receptor α gene expression in reproduction-related behaviors in female mice. *Endocrinology*. 1998;139(12):5070–5081.
7. **Dewing P, Boulware MI, Sinchak K, Christensen A, Mermelstein PG, Micevych P.** Membrane estrogen receptor-α interactions with metabotropic glutamate receptor 1a modulate female sexual receptivity in rats. *J Neurosci*. 2007;27(35):9294–9300.
8. **Christensen A, Micevych P.** CAV1 siRNA reduces membrane estrogen receptor-α levels and attenuates sexual receptivity. *Endocrinology*. 2012;153(8):3872–3877.
9. **Jensen EV, Greene GL, Closs LE, DeSombre ER, Nadji M.** Receptors reconsidered: a 20-year perspective. In: Greep RO, ed. *Recent Progress in Hormone Research*. Vol 38. New York: Academic; 1982;38:1–34.
10. **Green S, Chambon P.** A superfamily of potentially oncogenic hormone receptors. *Nature*. 1986;324(6098):615–617.
11. **Green S, Kumar V, Theulaz I, Wahli W, Chambon P.** The N-terminal DNA-binding 'zinc finger' of the oestrogen and glucocorticoid receptors determines target gene specificity. *EMBO J*. 1988;7(10):3037–3044.
12. **Webster NJ, Green S, Jin JR, Chambon P.** The hormone-binding domains of the estrogen and glucocorticoid receptors contain an inducible transcription activation function. *Cell*. 1988;54(2):199–207.
13. **Kumar V, Green S, Stack G, Berry M, Jin JR, Chambon P.** Functional domains of the human estrogen receptor. *Cell*. 1987;51(6):941–951.
14. **Krust A, Green S, Argos P, et al.** The chicken oestrogen receptor sequence: homology with v-erbA and the human oestrogen and glucocorticoid receptors. *EMBO J*. 1986;5(5):891–897.
15. **Grove-Strawser D, Boulware MI, Mermelstein PG.** Membrane estrogen receptors activate the metabotropic glutamate receptors mGluR5 and mGluR3 to bidirectionally regulate CREB phosphorylation in female rat striatal neurons. *Neuroscience*. 2010;170(4):1045–1055.
16. **Boulware MI, Weick JP, Becklund BR, Kuo SP, Groth RD, Mermelstein PG.** Estradiol activates group I and II metabotropic glutamate receptor signaling, leading to opposing influences on cAMP response element-binding protein. *J Neurosci*. 2005;25(20):5066–5078.
17. **Chaban VV, Lakhter AJ, Micevych P.** A membrane estrogen receptor mediates intracellular calcium release in astrocytes. *Endocrinology*. 2004;145(8):3788–3795.
18. **Micevych PE, Chaban V, Ogi J, Lakhter A, Lu JKH, Sinchak K.** Estradiol stimulates progesterone synthesis in hypothalamic astrocyte cultures. *Endocrinology*. 2007;148:782–789.
19. **Dewing P, Christensen A, Bondar G, Micevych P.** Protein kinase C signaling in the hypothalamic arcuate nucleus regulates sexual receptivity in female rats. *Endocrinology*. 2008;149(12):5934–5942.
20. **Eckersell CB, Popper P, Micevych PE.** Estrogen-induced alteration of μ-opioid receptor immunoreactivity in the medial preoptic nucleus and medial amygdala. *J Neurosci*. 1998;18:3967–3976.
21. **McGinnis MY, Krey LC, MacLusky NJ, McEwen BS.** Steroid receptor levels in intact and ovariectomized estrogen-treated rats: an examination of quantitative, temporal and endocrine factors influencing the efficacy of an estradiol stimulus. *Neuroendocrinology*. 1981;33(3):158–165.
22. **Parsons B, MacLusky NJ, Kreiger MS, McEwen BS, Pfaff DW.** The effects of long-term estrogen exposure on the induction of sexual behavior and measurements of brain estrogen and progestin receptors in the female rat. *Horm Behav*. 1979;13:301–313.
23. **Bondar G, Kuo J, Hamid N, Micevych P.** Estradiol-induced estrogen receptor-α trafficking. *J Neurosci*. 2009;29(48):15323–15330.
24. **Sinchak K, Romeo HE, Micevych PE.** Site-specific estrogen adn progestin regulation of orphanin FQ/nociceptin and nociceptin opioid receptor mRNA expression in the female rat limbic hypothalamic system. *J Comp Neurol*. 2006;496(2):252–268.
25. **Dominguez R, Micevych P.** Estradiol rapidly regulates membrane estrogen receptor α levels in hypothalamic neurons. *J Neurosci*. 2010;30(38):12589–12596.
26. **Mills RH, Sohn RK, Micevych PE.** Estrogen-induced μ-opioid receptor internalization in the medial preoptic nucleus is mediated via

neuropeptide Y-Y1 receptor activation in the arcuate nucleus of female rats. *J Neurosci*. 2004;24(4):947–955.
27. **Shughrue PJ, Bushnell CD, Dorsa DM.** Estrogen receptor messenger ribonucleic acid in female rat brain during the estrous cycle—a comparison with ovariectomized females and intact males. *Endocrinology*. 1992;131(1):381–388.
28. **Shughrue PJ, Lane MV, Merchenthaler I.** Comparative distribution of estrogen receptor-α and -β mRNA in the rat central nervous system. *J Comp Neurol*. 1997;388(4):507–525.
29. **Blaustein JD.** Estrogen receptor immunoreactivity in rat brain: rapid effects of estrodiol injection. *Endocrinology*. 1993;132:1218–1224.
30. **Brown TJ, Naftolin F, Maclusky NJ.** Sex differences in estrogen receptor binding in the rat hypothalamus: effects of subsaturating pulses of estradiol. *Brain Res*. 1992;578(1–2):129–134.
31. **Lauber A, Romano G, Mobbs C, Pfaff D.** Estradiol regulation of estrogen receptor mRNA in rat mediobasal hypothalamus: an in situ hybridization study. *J Neuroendocrinol*. 1990;2:605–611.
32. **Lauber A, Mobbs C, Muramatsu M, Pfaff D.** Estrogen receptor mRNA expression in the rat hypothalamus as a function of genetic sex and estrogen dose. *Endocrinology*. 1991;129:3180–3186.
33. **Greco B, Allegretto EA, Tetel MJ, Blaustein JD.** Coexpression of ER β with ER α and progestin receptor proteins in the female rat forebrain: effects of estradiol treatment. *Endocrinology*. 2001;142(12):5172–5181.
34. **Papka RE, Storey-Workley M, Shughrue PJ, et al.** Estrogen receptor-α and -β immunoreactivity and mRNA in neurons of sensory and autonomic ganglia and spinal cord. *Cell Tissue Res*. 2001;304(2):193–214.
35. **Sinchak K, Wagner EJ.** Estradiol signaling in the regulation of reproduction and energy balance. *Front Neuroendocrinol*. 2012;33(4):342–363.
36. **Borgquist A, Kachani M, Tavitian N, Sinchak K, Wagner EJ.** Estradiol negatively modulates the pleiotropic actions of orphanin FQ/nociceptin at proopiomelanocortin synapses [published online July 2, 2013]. *Neuroendocrinology*. doi:10.1159/000351868.
37. **Dominguez R, Dewing P, Kuo J, Micevych P.** Membrane-initiated estradiol signaling in immortalized hypothalamic N-38 neurons. *Steroids*. 2013;78(6):607–613.
38. **Razandi M, Pedram A, Greene G, Levin E.** Cell membrane and nuclear estrogen receptors (ERs) originate from a single transcript: studies of ERα and ERβ expressed in Chinese hamster ovary cells. *Mol Endocrinol*. 1999;13(2):307–319.
39. **Boulware MI, Kordasiewicz H, Mermelstein PG.** Caveolin proteins are essential for distinct effects of membrane estrogen receptors in neurons. *J Neurosci*. 2007;27(37):9941–9950.
40. **Schnitzer JE, McIntosh DP, Dvorak AM, Liu J, Oh P.** Separation of caveolae from associated microdomains of GPI-anchored proteins. *Science*. 1995;269(5229):1435–1439.
41. **Schnitzer JE, Liu J, Oh P.** Endothelial caveolae have the molecular transport machinery for vesicle budding, docking, and fusion including VAMP, NSF, SNAP, annexins, and GTPases. *J Biol Chem*. 1995;270(24):14399–14404.
42. **Garcia-Segura LM, Olmos G, Tranque P, Naftolin F.** Rapid effects of gonadal steroids upon hypothalamic neuronal membrane ultrastructure. *J Steroid Biochem*. 1987;27(1–3):615–623.
43. **Olmos G, Aguilera P, Tranque P, Naftolin F, Garcia-Segura LM.** Estrogen-induced synaptic remodelling in adult rat brain is accompanied by the reorganization of neuronal membranes. *Brain Res*. 1987;425(1):57–64.
44. **Parducz A, Szilagyi T, Hoyk S, Naftolin F, Garcia-Segura LM.** Neuroplastic changes in the hypothalamic arcuate nucleus: the estradiol effect is accompanied by increased exoendocytotic activity of neuronal membranes. *Cell Mol Neurobiol*. 1996;16(2):259–269.
45. **Moats RK 2nd, Ramirez VD.** Rapid uptake and binding of estradiol-17β-6-(O-carboxymethyl)oxime:125I-labeled BSA by female rat liver. *Biol Reprod*. 1998;58(2):531–538.
46. **Acconcia F, Ascenzi P, Bocedi A, et al.** Palmitoylation-dependent estrogen receptor α membrane localization: regulation by 17β-estradiol. *Mol Biol Cell*. 2005;16(1):231–237.
47. **Razandi M, Oh P, Pedram A, Schnitzer J, Levin ER.** ERs associate with and regulate the production of caveolin: implications for signaling and cellular actions. *Mol Endocrinol*. 2002;16(1):100–115.
48. **Pedram A, Razandi M, Sainson RC, Kim JK, Hughes CC, Levin ER.** A conserved mechanism for steroid receptor translocation to the plasma membrane. *J Biol Chem*. 2007;282(31):22278–22288.
49. **Lu KH, Hopper BR, Vargo TM, Yen SS.** Chronological changes in sex steroid, gonadotropin and prolactin secretions in aging female rats displaying different reproductive states. *Biol Reprod*. 1979;21(1):193–203.
50. **Day JR, Morales TH, Lu JK.** Male stimulation of luteinizing hormone surge, progesterone secretion and ovulation in spontaneously persistent-estrous, aging rats. *Biol Reprod*. 1988;38(5):1019–1026.
51. **Powers JB.** Hormonal control of sexual receptivity during the estrous cycle of the rat. *Physiol Behav*. 1970;5:831–835.
52. **Paxinos G, Watson C.** *The Rat Brain in Stereotaxic Coordinates*. 4th ed. San Diego: Academic Press; 1998.